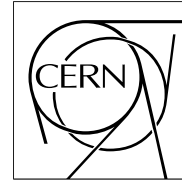


The Compact Muon Solenoid Experiment

# CMS Note

Mailing address: CMS CERN, CH-1211 GENEVA 23, Switzerland



May 18, 2001

## Investigations of operating scenarios for the sensors of the CMS silicon Tracker

E. Migliore<sup>a)</sup>

*CERN, Geneva, Switzerland*

### Abstract

The existing parametrizations for the annealing of the bulk damage induced by radiation in silicon are used to investigate the behaviour of depletion voltage, leakage current and power dissipation in different scenarios of operation during data-taking, shutdown and maintenance periods, of the Inner and of the Outer silicon Tracker of CMS.

---

<sup>a)</sup> Now at Dipartimento di Fisica Sperimentale, Università di Torino, Torino, Italy

# 1 Introduction

Among the main macroscopic effects of bulk damage induced by radiation in silicon detectors are the change of the effective charge carriers concentration, and therefore of the voltage required for full depletion, and the increase in the leakage current [1]. Measurements performed on diodes have shown that the time evolution of these effects largely depends on the temperature at which the sensors are kept after irradiation. Models have been developed to describe the annealing behaviour. Because of the high irradiation environment, the temperature of the sensors during the data-taking, which represents about 50 % of the sensors lifetime, has to be well below 0 °C to avoid the thermal runaway of the leakage current and to limit the power dissipated by the sensors themselves. On the contrary some freedom exists on the temperature at which the sensors have to be kept during shutdown periods and on the effects of maintenance interventions performed at room temperature. In this note the annealing models are used to discuss how different conditions for the operation of the sensors of the CMS silicon Tracker, during the periods of data-taking, shutdown and maintenance, will affect depletion voltage, leakage current and power dissipation during the lifetime of the experiment.

## 2 Fluences in the Tracker

The neutron ( $E > 100$  keV) and charged hadron fluences ( $\Phi_n$  and  $\Phi_p$  respectively) in the Tracker volume at the goal luminosity of  $5 \times 10^5 \text{pb}^{-1}$  are shown in figure 1.

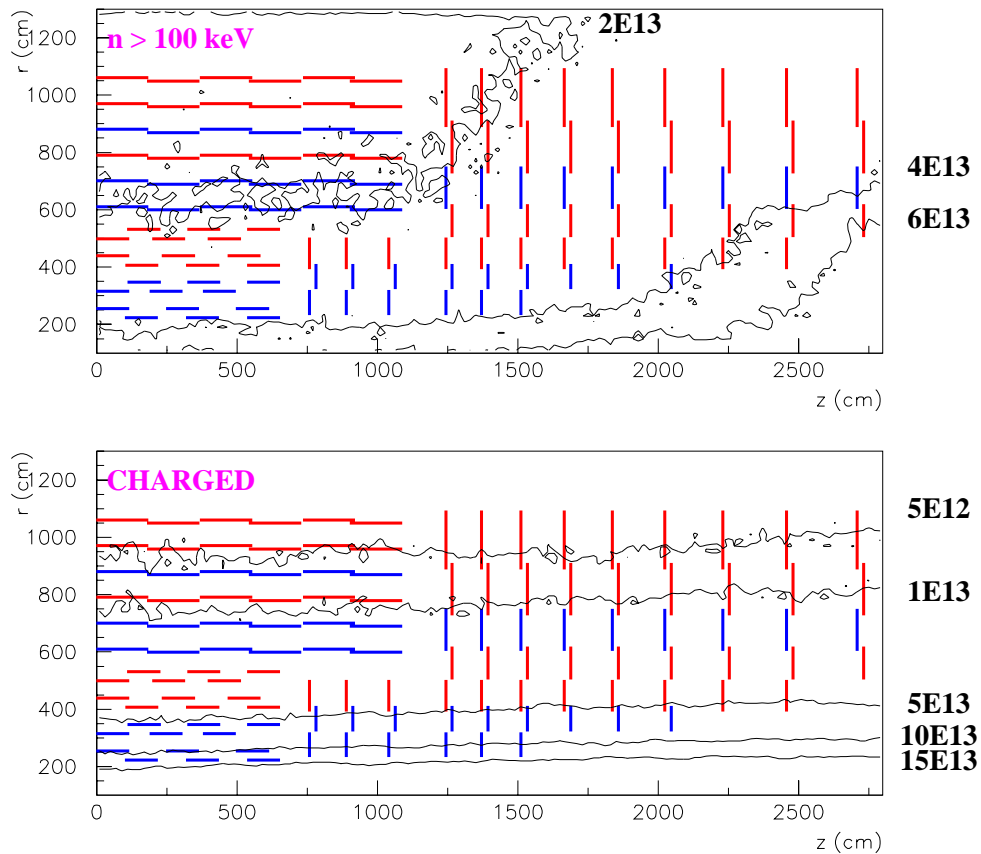


Figure 1: Neutron ( $E > 100$  keV) and charged hadron fluences in the Tracker volume in units of  $\text{cm}^{-2}$ . Double side modules are shown in blue, single side in red.

The sum of the two components is shown in figure 2 while figure 3 shows the number of modules versus the module total average fluence.

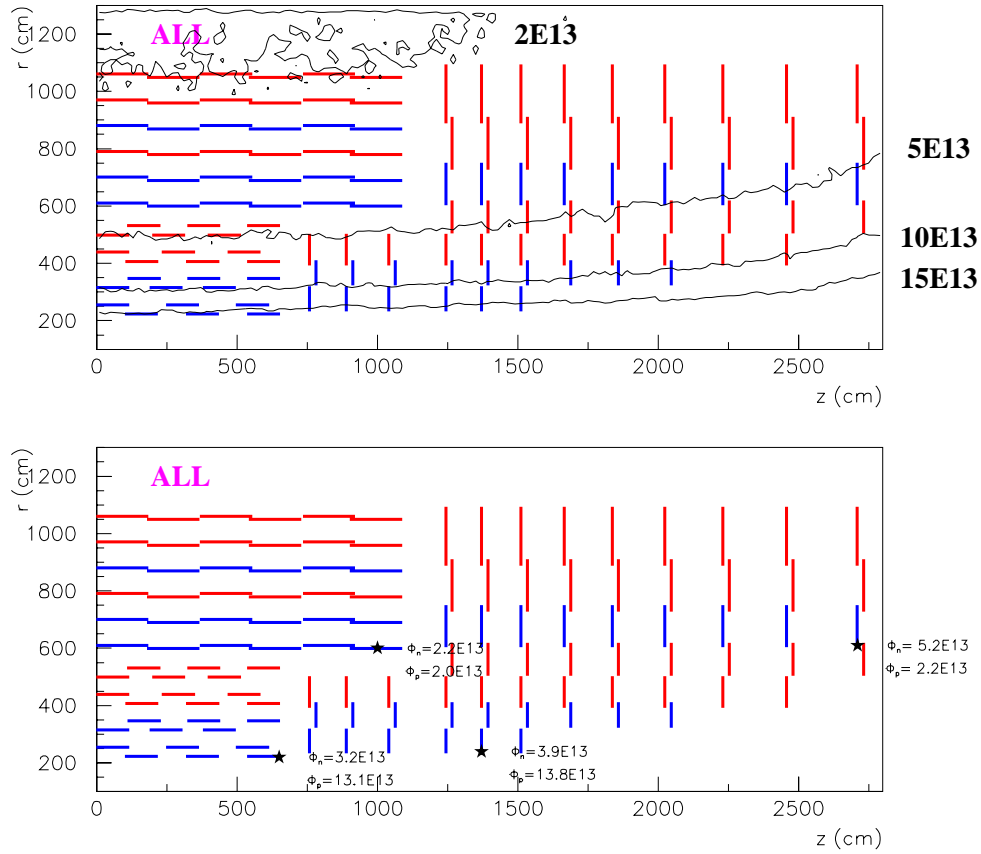


Figure 2: Top: Sum of neutron ( $E > 100$  keV) and charged hadron fluences in the Tracker volume in units of  $\text{cm}^{-2}$ . Double side modules are shown in blue, single side in red. Bottom: Points (stars) with the highest total fluence in the Inner Barrel, Inner Endcap, Outer Barrel and Outer Endcap together with their expected fluences.

In the following 4 different regions of the Tracker will be considered:

- Inner Barrel:  $r < 60$  cm,  $|z| < 110$  cm;
- Inner Endcap:  $r < 60$  cm,  $|z| > 110$  cm;
- Outer Barrel:  $60 < r < 110$  cm,  $|z| < 110$  cm;
- Outer Endcap:  $60 < r < 110$  cm,  $|z| > 110$  cm.

The values of the average  $\Phi_n$  and  $\Phi_p$  in the module with the largest total fluence for each of the four regions are shown in table 1. In the table the two components in the point of the module with the highest fluence are also shown. Fast variation of the charged hadron fluence across the module can be noted in case of the Inner Endcap region.

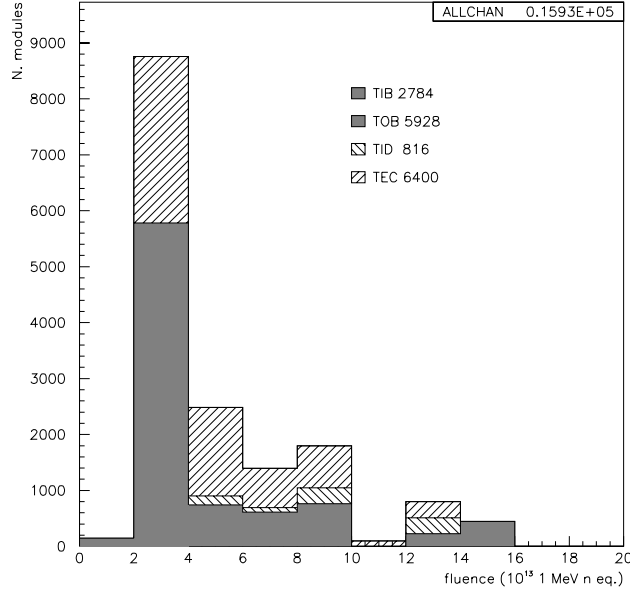


Figure 3: Number of modules as a function of the average total fluence,  $\langle\Phi_n\rangle + \langle\Phi_p\rangle$ , in units of  $10^{13} \text{ cm}^{-2}$ . Two entries were associated for each double side module.

Region	Module with highest $\langle\Phi_n\rangle + \langle\Phi_p\rangle$	Module with highest $\Phi_n + \Phi_p$
Inner Barrel	$r = 22 \text{ cm}$ $\langle\Phi_n\rangle = 3.3$ $z = 59 \text{ cm}$ $\langle\Phi_p\rangle = 12.6$	$r = 22 \text{ cm}$ $\max \Phi_n = 3.2$ $z = 65 \text{ cm}$ $\max \Phi_p = 13.1$
Inner Endcap	$r = 28 \text{ cm}$ $\langle\Phi_n\rangle = 3.5$ $z = 137 \text{ cm}$ $\langle\Phi_p\rangle = 10.2$	$r = 24 \text{ cm}$ $\max \Phi_n = 3.9$ $z = 137 \text{ cm}$ $\max \Phi_p = 13.8$
Outer Barrel	$r = 60 \text{ cm}$ $\langle\Phi_n\rangle = 2.1$ $z = 99 \text{ cm}$ $\langle\Phi_p\rangle = 1.8$	$r = 60 \text{ cm}$ $\max \Phi_n = 2.2$ $z = 100 \text{ cm}$ $\max \Phi_p = 2.0$
Outer Endcap	$r = 68 \text{ cm}$ $\langle\Phi_n\rangle = 4.0$ $z = 271 \text{ cm}$ $\langle\Phi_p\rangle = 1.6$	$r = 61 \text{ cm}$ $\max \Phi_n = 5.2$ $z = 271 \text{ cm}$ $\max \Phi_p = 2.2$

Table 1: Average neutron  $\Phi_n$  and charge hadron  $\Phi_p$  fluences, at  $5 \times 10^5 \text{ pb}^{-1}$ , in the modules with the highest total average fluence for different Tracker regions. In the last column the two components in the point with highest fluence of the module are indicated. Fluences are in units of  $10^{13} \text{ cm}^{-2}$ .

Instantaneous fluence is proportional to instantaneous luminosity. In this note the nominal instantaneous luminosity was assumed to be  $\mathcal{L} = 0.5 \times 10^{35} \text{ cm}^{-2} \text{ s}^{-1}$ , corresponding to one fill about 12 hours long per day, and the delivered fraction of the nominal luminosity was assumed to be [2]:

- 10 % in the first year;
- 33 % in the second year;
- 67 % in the third year;
- 100 % from fourth year on.

With these assumptions the goal integrated luminosity of  $5 \times 10^5 \text{ pb}^{-1}$  is reached after about 3000 days after the start of data taking.

At present uncertainty factors of 2.0 and 1.3 should be assumed on  $\Phi_n$  and  $\Phi_p$  respectively. The monitoring during data-taking of the leakage current of the sensors, which is proportional to the actual fluence in the experiment (cf. below Section 8), will surely help in reducing these uncertainties.

### 3 Model of the depletion voltage variations

The evolution of the effective charge carriers concentration  $N_{eff}$  in an irradiated silicon sensor is described by the so called *Hamburg Model* [1, 3]. According to it, the value of  $N_{eff}$  for a sensor exposed to a “quantum” of radiation  $\Delta\Phi$  at the time  $t = 0$ , evolves at the time  $t$  and at the temperature  $T$  as:

$$N_{eff}(\Delta\Phi, T, t) = N_{eff,0} - \Delta N_{eff}(\Delta\Phi, T, t)$$

where:

$$\Delta N_{eff}(\Delta\Phi, T, t) = N_C(\Delta\Phi) + N_A(\Delta\Phi, T, t) + N_Y(\Delta\Phi, T, t) \quad (1)$$

It was assumed  $N_{eff,0}$  to be positive in a  $n$ -type not irradiated silicon substrate.

The three terms on RHS correspond to *short term annealing*:

$$N_A(\Delta\Phi, T, t) = g_A \Delta\Phi e^{-t/\tau_A} \quad (2)$$

*reverse annealing*<sup>1)</sup>:

$$N_Y(\Delta\Phi, T, t) = g_Y \Delta\Phi \left(1 - e^{-t/\tau_Y}\right) \quad (3)$$

*acceptor introduction and donor removal* (together indicated as *stable damage*):

$$N_C(\Delta\Phi) = g_C \Delta\Phi + N_{C,0} (1 - e^{-c\Delta\Phi}) \quad (4)$$

In eq. 4 the removal constant  $c$  and the removable initial donor concentration  $N_{C,0}$  are not independent:  $N_{C,0} \times c = \mathcal{O}(10^{-1}) \text{ cm}^{-1}$  and  $N_{C,0}/N_{eff,0} = r_C$ .

Temperature dependence is introduced in eq. 2 and 3 by the time constants of beneficial and reverse annealing which obey Arrhenius relations (see fig. 4):

$$\tau_A^{-1}(T) = k_A = k_{A,0} e^{-E_{aA}/k_B T} \quad \text{and} \quad \tau_Y^{-1}(T) = k_Y = k_{Y,0} e^{-E_{aY}/k_B T}$$

with  $k_B$  the Boltzmann’s constant. The input values used in the computations are summarized in tables 2 (annealing) and 3 (stable damage) for neutrons and charged hadrons (indicated shortly in the following as *proton*) separately.

		n	p
$g_A$	( $\text{cm}^{-1}$ )	$(1.81 \pm 0.14) \times 10^{-2}$	
$k_{A,0}$	( $\text{s}^{-1}$ )	$(2.4_{-0.8}^{+1.2}) \times 10^{13}$	
$E_{aA}$	(eV)	$1.09 \pm 0.03$	
$g_Y$	( $\text{cm}^{-1}$ )	$5.2 \times 10^{-2}$	$6.6 \times 10^{-2}$
$k_{Y,0}$	( $\text{s}^{-1}$ )	$(1.5_{-1.1}^{+3.4}) \times 10^{15}$	
$E_{aY}$	(eV)	$1.33 \pm 0.03$	

Table 2: Parameters for the annealing of the Hamburg Model used in this simulation.

		n	p
$g_C$	( $\text{cm}^{-1}$ )	$1.5 \times 10^{-2}$	$1.9 \times 10^{-2}$
$N_{eff,0} \times c$	( $\text{cm}^{-1}$ )	$10.9 \times 10^{-2}$	
$r_C$		0.7	1.0

Table 3: Parameters for the stable damage of the Hamburg Model used in this simulation.

From  $N_{eff}$  the depletion voltage was then computed as:

$$V_{dep} = \frac{|eN_{eff}|d^2}{2\varepsilon_0\varepsilon_{Si}}$$

with  $d$  the sensor thickness.

<sup>1)</sup> The relation is strictly valid for standard silicon devices as in the case of the oxygenated ones saturation effects on  $N_Y$  with the fluence have been observed.

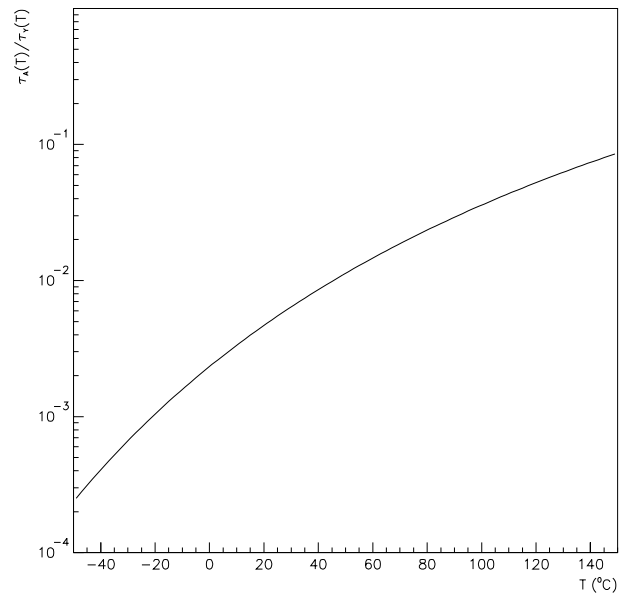
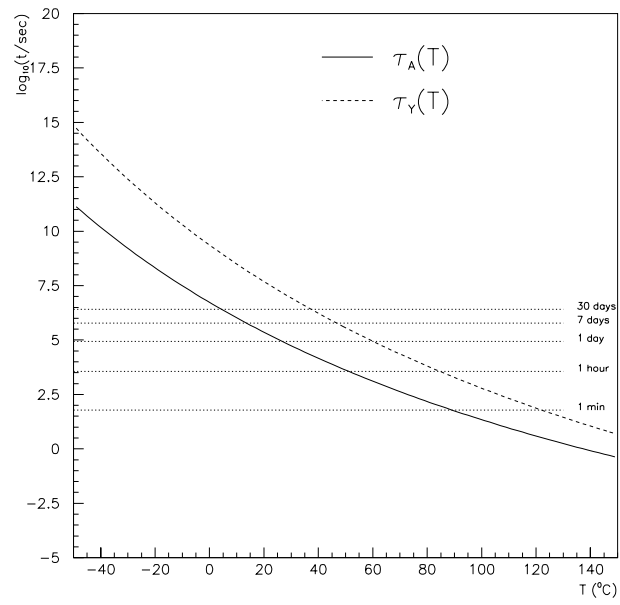


Figure 4: Top: temperature evolution of the time constants  $\tau_A$  and  $\tau_Y$ . Bottom: ratio  $\tau_A/\tau_Y$  as a function of temperature.

The scenario for LHC operations during each year was assumed to be (in days) [2]:

- *data-taking*: 60 (run) - 14 (stand-by) - 60 (run) - 14 (stand-by) - 60 (run) at temperature  $T_{dt}$ ;
- *shutdown*: 157 at temperature  $T_{sd}$ .

The model was applied for the simulation as follows:

- the expected fluence corresponding to  $5 \times 10^5 \text{pb}^{-1}$  was divided into *irradiation chunks* of  $\Delta t = 12$  hours. The radiation content  $\Delta\Phi_i$  in the chunk  $[t_{i-1}, t_i]$  was taken proportional to the integrated luminosity in that time slot;
- the  $\Delta N_{eff}(\Delta\Phi_i)$  for the chunks at times  $t_j \geq t_i$  were obtained according to eq. 1;
- the total  $\Delta N_{eff}$  at a time  $t_j$  was computed summing up the  $\Delta N_{eff,i}$  contributions from the chunks with  $t_i < t_j$  after computing the time evolution as explained in the previous point.

One of the largest uncertainties in the Hamburg model is the implementation of the donor removal mechanism, as data with neutron irradiation shows that a fraction of the initial dopant concentration  $[P]_0 = N_{eff,0}$  is left even at the highest doses. The situation is more confused for proton irradiation as some of the groups observe complete donor removal while other do not. Moreover no data on the effects of combined neutron and proton irradiation exists. For this simulation the following procedure was followed: the initial donor concentration was decreased after each irradiation chunk according to the prescription of eq. 4 adding together the contributions of neutron and proton fluence. The donor removal due to proton or neutron was then stopped at the step  $j$ -th if the donor concentration became  $[P]_j < r_{C,k}[P]_0$  ( $k=p,n$ ).

## 4 Inner Tracker

The fluences for hottest modules of the Inner Tracker are:

- Barrel  
n fluence:  $\Phi_n = 3.3 \times 10^{13} \text{ 1-MeV n/cm}^{-2}$   
p fluence:  $\Phi_p = 12.6 \times 10^{13} \text{ 1-MeV n/cm}^{-2}$
- Endcap  
n fluence:  $\Phi_n = 3.5 \times 10^{13} \text{ 1-MeV n/cm}^{-2}$   
p fluence:  $\Phi_p = 10.2 \times 10^{13} \text{ 1-MeV n/cm}^{-2}$

The sensors for the Inner Tracker will have bulk resistivity  $\rho = 1.5 - 3 \text{ k}\Omega\text{cm}$  and thickness  $d = 320 \mu\text{m}$  [4]. Sensors will undergo to type inversion and the maximum bias voltage in the hottest zones will be reached at the end of the LHC run.

The analysis of the model predictions for these sensors hints to the fact that, because of the high radiation environment, the inversion point will be reached after a time which is almost independent on the sensor temperature but that depends heavily on the assumptions on the donor removal mechanism. Therefore one could expect that the final  $V_{dep}$  will be sensitive mainly to the temperature at which the sensor will stay after the type inversion.

**Evaluation of the time of the type inversion** The following scenarios were considered:

- two different temperatures for the sensors during the data-taking ( $T_{dt}$ ). In both the cases a temperature below  $0^\circ\text{C}$  was required because of the leakage current (cf. Section 8) and not for the annealing behaviour;
- for each  $T_{dt}$ , the time of the type inversion was evaluated in the case of two different temperatures  $T_{sd}$  for the shutdown periods:  $T_{sd} = T_{dt}$  (“no intervention” case) and  $T_{sd} = +20^\circ\text{C}$  (“major repair” case);
- the uncertainties in the donor removal by protons were evaluated considering the two cases:  $r_{C,p} = 1$  (“complete donor removal”) and  $r_{C,p} = 0.5$  (“partial donor removal”)

$T_{dt} = -20^\circ\text{C}$	Barrel		Endcap	
$T_{sd}$	$-20^\circ\text{C}$	$+20^\circ\text{C}$	$-20^\circ\text{C}$	$+20^\circ\text{C}$
$r_{C,p} = 1.0$	769	765	808	795
$r_{C,p} = 0.5$	825	818	852	845

Table 4: Inner Tracker: time (in days) of type inversion after start of LHC run, at  $T_{dt} = -20^\circ\text{C}$ .

$T_{dt} = -10^\circ\text{C}$	Barrel		Endcap	
$T_{sd}$	$-10^\circ\text{C}$	$+20^\circ\text{C}$	$-10^\circ\text{C}$	$+20^\circ\text{C}$
$r_{C,p} = 1.0$	784	766	826	806
$r_{C,p} = 0.5$	856	821	901	850

Table 5: Inner Tracker: time (in days) of type inversion after start of LHC run, at  $T_{dt} = -10^\circ\text{C}$ .

The worst scenario was in correspondence to fastest reach of the type inversion: therefore the simulation was performed for  $\rho = 3 \text{ k}\Omega\text{cm}$  (upper limit for accepted resistivities).

Results are shown in tables 4 and 5. It can be noted that the worst scenario, fastest reach of inversion point, is obtained for the model with  $r_{C,p} = 1$ . Therefore this conservative assumption was taken in the following step.

**Evaluation of  $V_{dep}$  after  $5 \times 10^5 \text{ pb}^{-1}$**  Tables 4 and 5 show that the time of the type-inversion does not depend too much on the temperature  $T_{sd}$  of the shutdowns before type inversion itself. On the contrary one expects that the  $V_{dep}$  at the end of LHC run will depend highly on the temperature of the shutdowns after type inversion. Therefore, for each  $T_{dt}$ , different combinations of shutdown temperatures before ( $T_{sd}$ ) and after ( $T_{sd,after}$ ) the type inversion were considered. The predicted  $V_{dep}$  at the end of LHC run are shown in table 6 ( $T_{dt} = -20^\circ\text{C}$ ) and table 7 ( $T_{dt} = -10^\circ\text{C}$ ).

**Implications for the operations of the Inner Tracker** From tables 6 and 7 one can extract the  $V_{dep}$  at the end of LHC run for sensors kept always at the lowest temperature:

- $T_{dt} = T_{sd} = T_{sd,after} = -20^\circ\text{C}$   
 $\rightarrow V_{dep} = 365 \text{ V}$  (barrel) and  $V_{dep} = 315 \text{ V}$  (endcap);
- $T_{dt} = T_{sd} = T_{sd,after} = -10^\circ\text{C}$   
 $\rightarrow V_{dep} = 265 \text{ V}$  (barrel) and  $V_{dep} = 225 \text{ V}$  (endcap);

In the case of  $T = -20^\circ\text{C}$ , operations of the sensors for some time at higher temperature could be even envisaged to profit of the beneficial annealing while the case of  $T = -10^\circ\text{C}$  is already close to the optimal operation temperature.

For what concerns scenarios of possible interventions two different cases were considered :

1. interventions before type inversion took place: the comparison of the columns  $T_{sd} = -20^\circ\text{C}$  and  $T_{sd} = +20^\circ\text{C}$  in tables 6 and 7 shows that opposite shutdown temperatures before type inversion result in difference on the  $V_{dep}$  at the end of the LHC run in the range 10-20 V.
2. interventions both before and after type inversion: it was assumed that the intervention implied 21 days at  $+20^\circ\text{C}$  (“extraction from CMS”) and 14 days at  $+10^\circ\text{C}$  (“repair in the lab”). Table 8 shows the expected  $V_{dep}$  after  $5 \times 10^5 \text{ pb}^{-1}$  for interventions in different years. As anticipated, in case of data-taking at  $T_{dt} = -20^\circ\text{C}$ , interventions at high temperature result in a decrease of the final  $V_{dep}$  because of the beneficial annealing. However later interventions give in general better  $V_{dep}$  performances. On the contrary, in the case of data-taking at  $T_{dt} = -10^\circ\text{C}$ , interventions at high temperature always result in a higher final  $V_{dep}$ . Comparing the “1+3”, “1+5” and “1+7” scenarios at  $T_{dt} = -10^\circ\text{C}$  it can be noted that scenarios with earlier interventions will lead to lower final  $V_{dep}$ , as the amount of absorbed dose which reverse anneals is smaller.

$T_{sd}$	Barrel		Endcap	
	-20 °C	+20 °C	-20 °C	+20 °C
$T_{sd,after} = -20^\circ \text{ C}$	365	375	315	320
$T_{sd,after} = -10^\circ \text{ C}$	290	305	245	260
$T_{sd,after} = 0^\circ \text{ C}$	255	270	215	230
$T_{sd,after} = +10^\circ \text{ C}$	340	350	290	300
$T_{sd,after} = +20^\circ \text{ C}$	665	670	570	570

Table 6: Inner Tracker:  $V_{dep}$  (in V) after  $5 \times 10^5 \text{ pb}^{-1}$  for  $T_{dt} = -20^\circ \text{ C}$ .

$T_{sd}$	Barrel		Endcap	
	-10 °C	+20 °C	-10 °C	+20 °C
$T_{sd,after} = -10^\circ \text{ C}$	265	275	225	235
$T_{sd,after} = 0^\circ \text{ C}$	255	270	220	230
$T_{sd,after} = +10^\circ \text{ C}$	340	350	290	300
$T_{sd,after} = +20^\circ \text{ C}$	665	670	570	570

Table 7: Inner Tracker:  $V_{dep}$  (in V) after  $5 \times 10^5 \text{ pb}^{-1}$  for  $T_{dt} = -10^\circ \text{ C}$ .

**Evaluation of systematics effects on annealing model** The  $V_{dep}$  after  $5 \times 10^5 \text{ pb}^{-1}$  were evaluated after changing independently the annealing parameters of the model by the errors indicated in table 2. In general the variations of  $V_{dep}$  due to the changes on  $g_A$  and  $g_Y$ <sup>2)</sup> are smaller than the effect due to the changes in  $(E_{aA}, k_{A,0})$  and  $(E_{aY}, k_{Y,0})$ . On the other hand the excursions of  $V_{dep}$  when  $k_{Y,0}$  is varied of its full error are similar to those obtained when  $E_{aY}$  is varied of its full error and similarly for  $E_{aA}$  and  $k_{A,0}$ . Table 9 shows the minimum and maximum values for  $V_{dep}$  obtained when changing the annealing parameters of their errors for the scenarios of table 8.

As expected, the most relevant parameter change for scenarios where the effect of the beneficial annealing is present, like “1+7” at  $T_{dt} = -20^\circ \text{ C}$ , is the variation of  $E_{aA}$  while for those where the long term annealing effects are relevant, like “1+3+5+7” at  $T_{dt} = -20^\circ \text{ C}$ , is the variation of  $E_{aY}$ . The differences between the “maximum” values of table 9 and the reference ones of table 8 are in the range 30-95 V. However the largest differences correspond to the most extreme running conditions. In the intermediate scenarios systematics of  $\pm 50 \text{ V}$  at  $T_{dt} = -20^\circ \text{ C}$  and  $\pm 60 \text{ V}$  at  $T_{dt} = -10^\circ \text{ C}$  can be assumed.

However the final  $V_{dep}$  is below 400 V for almost all the scenarios. Finally the monitoring of the annealing parameters on the sensors actually used in the experiment will surely reduce the systematics uncertainty.

**Evaluation of systematics effects due to the spread of the resistivities** The  $V_{dep}$  after  $5 \times 10^5 \text{ pb}^{-1}$  was evaluated changing the initial substrate resistivities from 1.5 to 3  $\text{k}\Omega\text{cm}$  (cf. figure 5). No significant variation was observed over the allowed range of  $\rho$  for all the intervention scenarios of table 8.

<sup>2)</sup>  $g_Y$  was changed of  $\pm 10\%$ , i.e. the same relative error as in the case of  $g_A$  was assumed.

year(s) of the intervention	$T_{dt} = -20^\circ\text{C}$		$T_{dt} = -10^\circ\text{C}$	
	Barrel	Endcap	Barrel	Endcap
1	365	315	265	225
1+3	360	305	270	230
1+5	330	285	275	235
1+7	295	250	280	240
1+3+5	335	290	280	240
1+3+7	280	255	285	245
1+3+5+7	310	265	300	255

Table 8: Inner Tracker:  $V_{dep}$  (in V) after  $5 \times 10^5 \text{pb}^{-1}$  for different intervention scenarios.

year(s) of the intervention			$T_{dt} = -20^\circ\text{C}$		$T_{dt} = -10^\circ\text{C}$	
			Barrel	Endcap	Barrel	Endcap
1	$E_{aA} = 1.06 \text{ eV}$	min	280	240	240	205
	$E_{aA} = 1.12 \text{ eV}$	max	420	360	335	285
1+3	$E_{aA} = 1.06 \text{ eV}$	min	285	245	245	210
	$E_{aA} = 1.12 \text{ eV}$	max	400	345	335	285
1+5	$E_{aA} = 1.06 \text{ eV}$	min	290	250	255	215
	$E_{aY} = 1.30 \text{ eV}$	max	365	315	320	275
1+7	$E_{aY} = 1.36 \text{ eV}$	min	275	235	260	220
	$E_{aY} = 1.30 \text{ eV}$	max	350	295	345	290
1+3+5	$E_{aA} = 1.06 \text{ eV}$	min	295	250	260	220
	$E_{aY} = 1.30 \text{ eV}$	max	380	325	335	285
1+3+7	$E_{aY} = 1.36 \text{ eV}$	min	275	235	260	225
	$E_{aY} = 1.30 \text{ eV}$	max	360	310	355	305
1+3+5+7	$E_{aY} = 1.36 \text{ eV}$	min	280	240	265	225
	$E_{aY} = 1.30 \text{ eV}$	max	400	345	395	335

Table 9: Inner Tracker: minimum and maximum  $V_{dep}$  (in V) after  $5 \times 10^5 \text{pb}^{-1}$  for different intervention scenarios, obtained with the parameter change indicated in the second column.

## 5 Outer Tracker

The fluences for hottest modules of the Outer Tracker are:

- Barrel  
n fluence:  $\Phi_n = 2.1 \times 10^{13} \text{ 1-MeV n/cm}^{-2}$   
p fluence:  $\Phi_p = 1.8 \times 10^{13} \text{ 1-MeV n/cm}^{-2}$
- Endcap  
n fluence:  $\Phi_n = 4.0 \times 10^{13} \text{ 1-MeV n/cm}^{-2}$   
p fluence:  $\Phi_p = 1.6 \times 10^{13} \text{ 1-MeV n/cm}^{-2}$

The sensors for the Outer Tracker will have bulk resistivity  $\rho = 3.5 - 6 \text{ k}\Omega\text{cm}$  and thickness  $d = 500 \mu\text{m}$  [4].

**Evaluation of the time of the type inversion** The same scenarios as for the Inner Tracker were considered:

- two different temperatures for the sensors during the data-taking ( $T_{dt}$ ), both below  $0^\circ\text{C}$ .
- for each  $T_{dt}$ , the time of the type inversion was evaluated in the case of two different temperatures  $T_{sd}$  for the shutdown periods:  $T_{sd} = T_{dt}$  (“no intervention” case) and  $T_{sd} = +20^\circ\text{C}$  (“major repair” case);
- only the case of complete donor removal by the protons,  $r_{C,p} = 1$ , was considered.

Once more the worst scenario is in correspondence to fastest reach of the type inversion: therefore the simulation was performed for  $\rho = 6 \text{ k}\Omega\text{cm}$  (upper limit for accepted resistivities). Results are shown in tables 10 and 11.

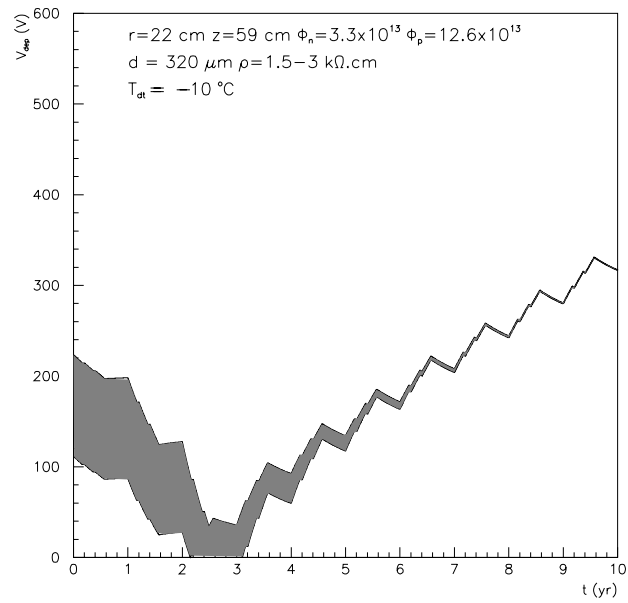
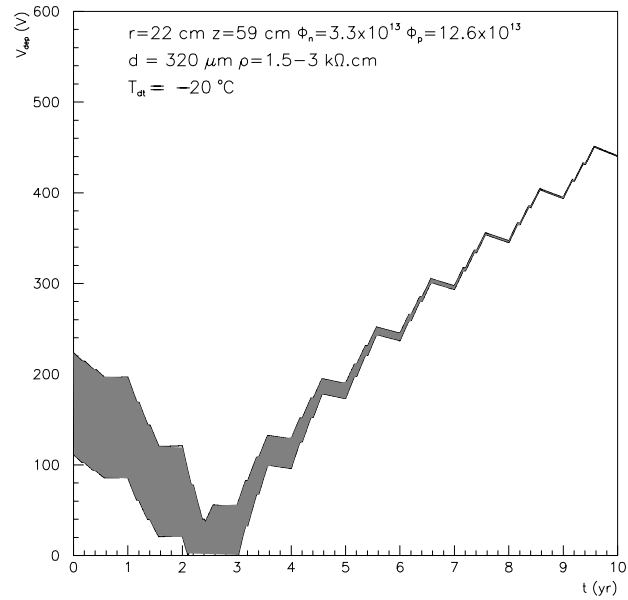


Figure 5: Depletion voltage as a function of time for a sensor in the hottest module of the Inner Barrel for the allowed range of initial resistivities. Data-taking temperature  $T_{dt} = -20^\circ\text{C}$  (top) and  $T_{dt} = -10^\circ\text{C}$  (bottom) and “no intervention” scenario.

$T_{dt} = -20^\circ\text{C}$	Barrel		Endcap	
$T_{sd}$	$-20^\circ\text{C}$	$+20^\circ\text{C}$	$-20^\circ\text{C}$	$+20^\circ\text{C}$
$r_{C,p} = 1.0$	1115	1103	854	852

Table 10: Outer Tracker: time (in days) of type inversion after start of LHC run, at  $T_{dt} = -20^\circ\text{C}$ .

$T_{dt} = -10^\circ\text{C}$	Barrel		Endcap	
$T_{sd}$	$-10^\circ\text{C}$	$+20^\circ\text{C}$	$-10^\circ\text{C}$	$+20^\circ\text{C}$
$r_{C,p} = 1.0$	1146	1103	894	856

Table 11: Outer Tracker: time (in days) of type inversion after start of LHC run, at  $T_{dt} = -10^\circ\text{C}$ .

**Evaluation of  $V_{dep}$  after  $5 \times 10^5 \text{pb}^{-1}$**  Also in the case of the Outer Tracker, for each  $T_{dt}$ , different combinations of shutdown temperatures before ( $T_{sd}$ ) and after ( $T_{sd,after}$ ) the type inversion were considered. The predicted  $V_{dep}$  at the end of LHC run are shown in table 12 ( $T_{dt} = -20^\circ\text{C}$ ) and table 13 ( $T_{dt} = -10^\circ\text{C}$ ).

**Implications for the operations of the Outer Tracker** From tables 12 and 13 one can extract the  $V_{dep}$  at the end of LHC run for sensors kept always at the lowest temperature:

- $T_{dt} = T_{sd} = T_{sd,after} = -20^\circ\text{C}$   
 $\rightarrow V_{dep} = 205 \text{ V}$  (barrel) and  $V_{dep} = 290 \text{ V}$  (endcap);
- $T_{dt} = T_{sd} = T_{sd,after} = -10^\circ\text{C}$   
 $\rightarrow V_{dep} = 145 \text{ V}$  (barrel) and  $V_{dep} = 200 \text{ V}$  (endcap);

The sensors of the Barrel Outer Tracker will require a  $V_{dep}$  at the end of the LHC safely below 400 V in all the scenarios investigated. This is true also in the case of the sensors of the Endcap Outer Tracker provided that a temperature not larger than  $10^\circ\text{C}$  is kept in the shutdown periods after type inversion. For completeness the  $V_{dep}$  at the end of the LHC run in the same intervention scenarios considered for the Inner Tracker are reported in table 14.

**Evaluation of systematic effects due to the spread of the resistivities** The  $V_{dep}$  after  $5 \times 10^5 \text{pb}^{-1}$  was evaluated changing the initial substrate resistivities from 3.5 to 6  $\text{k}\Omega\text{cm}$  (cf. table 15 and figure 6). Contrary to the case of the Inner Tracker, for the Outer Tracker the final  $V_{dep}$  is sensitive to the initial substrate resistivity and the range spanned is about 20 V.

$T_{sd}$	Barrel		Endcap	
	-20 °C	+20 °C	-20 °C	+20 °C
$T_{sd,after} = -20^\circ \text{C}$	205	220	290	295
$T_{sd,after} = -10^\circ \text{C}$	160	180	220	230
$T_{sd,after} = 0^\circ \text{C}$	135	160	190	200
$T_{sd,after} = +10^\circ \text{C}$	180	200	255	265
$T_{sd,after} = +20^\circ \text{C}$	360	370	505	505

Table 12: Outer Tracker:  $V_{dep}$  (in V) after  $5 \times 10^5 \text{pb}^{-1}$  for  $T_{dt} = -20^\circ \text{C}$ .

$T_{sd}$	Barrel		Endcap	
	-10 °C	+20 °C	-10 °C	+20 °C
$T_{sd,after} = -10^\circ \text{C}$	145	165	200	210
$T_{sd,after} = 0^\circ \text{C}$	135	160	190	200
$T_{sd,after} = +10^\circ \text{C}$	185	200	255	265
$T_{sd,after} = +20^\circ \text{C}$	360	370	505	505

Table 13: Outer Tracker:  $V_{dep}$  (in V) after  $5 \times 10^5 \text{pb}^{-1}$  for  $T_{dt} = -10^\circ \text{C}$ .

## 6 Different scenario for the delivered luminosity

An alternative scenario for the delivered luminosity was investigated assuming that LHC reaches the full nominal luminosity  $0.5 \times 10^{35} \text{cm}^{-2} \text{s}^{-1}$  already in the first year of operations. In this case the integrated luminosity of  $5 \times 10^5 \text{pb}^{-1}$  is reached after about 2300 days after the start of data taking. The required  $V_{dep}$  in the hottest points of Inner and Outer Tracker for the intervention scenarios of tables 8 and 14 are shown in tables 16 and 17 respectively <sup>3)</sup>. For a sensor temperature during data-taking  $T_{dt} = -20^\circ \text{C}$ ,  $V_{dep}$  is reduced from 5 to 25 V. For  $T_{dt} = -10^\circ \text{C}$ ,  $V_{dep}$  instead increases from 5 to 20 V in the case of the Inner Tracker, and up to 10 V in the case of the Outer. The decrease of the final  $V_{dep}$  observed for  $T_{dt} = -20^\circ \text{C}$ , can be explained recalling that, as shown previously, in this case the beneficial annealing is almost absent if no period at higher temperature takes place. All the scenarios examined have in common an intervention after the first year of operations. In the high luminosity run the fraction of the total dose which benefits of the annealing is therefore larger. Evolutions of  $V_{dep}$  as a function of time in the case of 1 intervention after the first year of data-taking, in the two LHC luminosity scenarios and for  $T_{dt} = -20^\circ \text{C}$  and  $T_{dt} = -10^\circ \text{C}$ , are shown in figure 7 and 8 for the Inner Barrel and Outer Endcap respectively.

## 7 Uncertainty on the fluence

The factor of uncertainty on expected fluences in the Tracker volume is about 2 for neutron and 1.3 for charged hadrons. In the case of the Inner Tracker (table 18), as  $\Phi_p \approx 3\Phi_n$ ,  $\Delta\Phi_p \approx \Delta\Phi_n$  and the change on the final  $V_{dep}$  from the uncertainty on the two fluences is similar. The effect is enhanced for a running temperature  $T_{dt} = -20^\circ \text{C}$  ( $\Delta V_{dep} \approx 70 \text{V}$ ) while it is reduced at  $T_{dt} = -10^\circ \text{C}$  ( $\Delta V_{dep} \approx 55 \text{V}$ ). In the case of the Outer Tracker (table 19)  $\Phi_n \geq \Phi_p$  and the uncertainty on the neutron fluence dominates. This is true in particular for the Outer Endcap where  $\Phi_n \approx 2\Phi_p$  and the variation of  $V_{dep}$  is up to 200 V while the uncertainty on  $\Phi_p$  results in an increase of  $V_{dep}$  of about 30 V. Concerning the comparison between the two running temperatures  $T_{dt}$ , similar considerations as for the Inner Tracker hold.

<sup>3)</sup> Since the goal luminosity is reached during the sixth year of operations, scenarios with interventions after the seventh year were not considered.

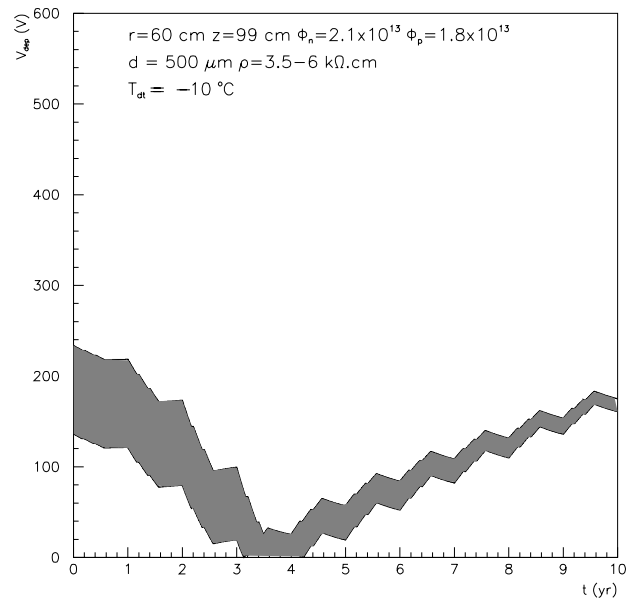
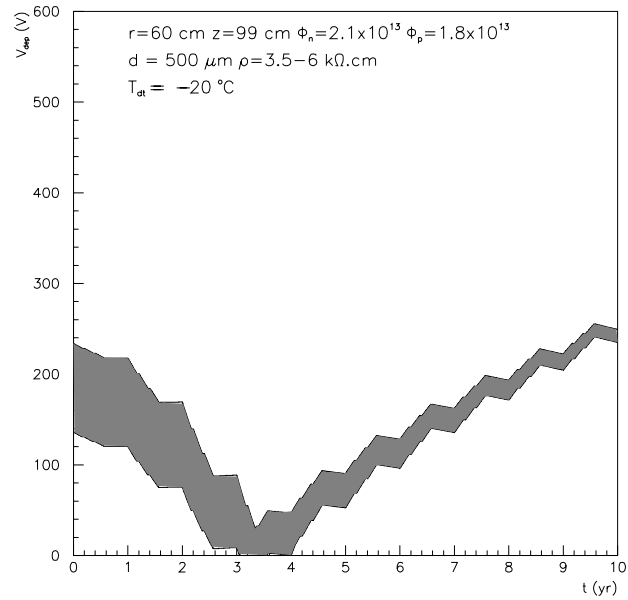


Figure 6: Depletion voltage as a function of time for a sensor in the hottest module of the Outer Barrel for the allowed range of initial resistivities. Data-taking temperature  $T_{dt} = -20^\circ\text{C}$  (top) and  $T_{dt} = -10^\circ\text{C}$  (bottom) and “no intervention” scenario.

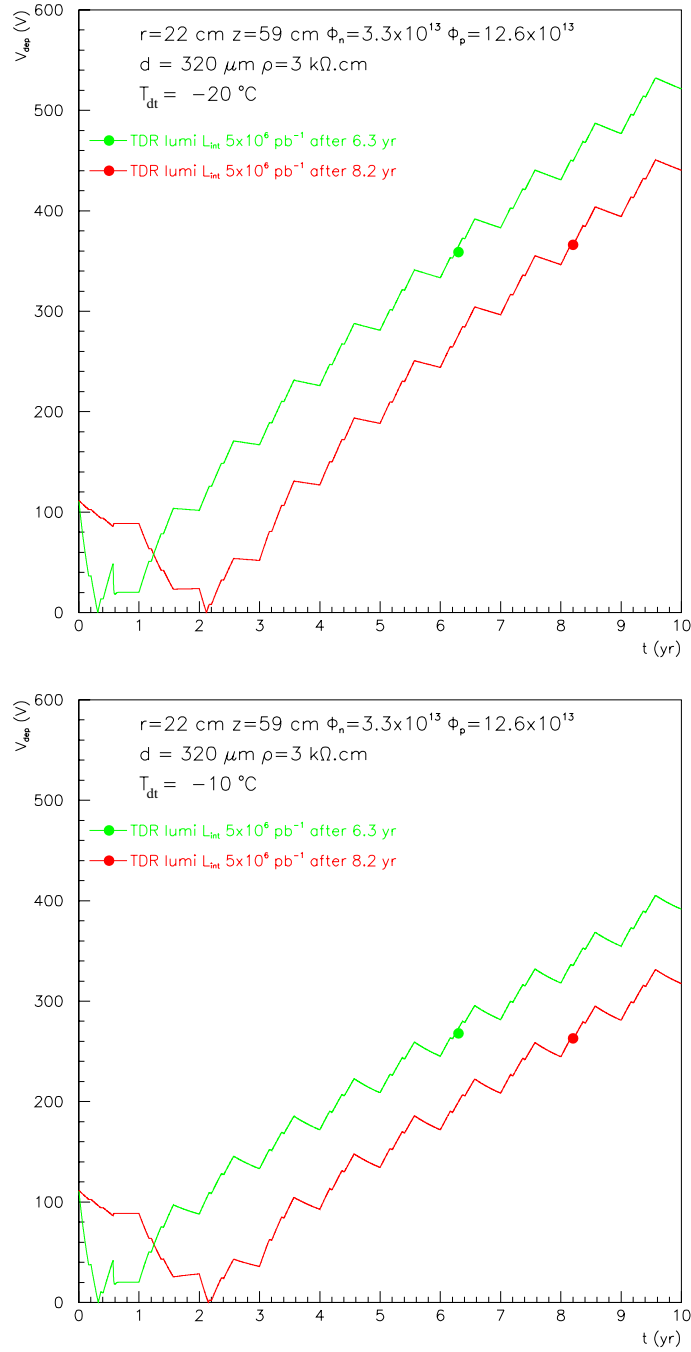


Figure 7: Depletion voltage as a function of time for a sensor in the hottest module of the Inner Barrel with one intervention after 1 year of data-taking (cf. table 8) and for two different luminosity scenarios (see text). Data-taking temperature  $T_{dt} = -20^\circ\text{C}$  (top) and  $T_{dt} = -10^\circ\text{C}$  (bottom). Dots correspond to  $5 \times 10^5\text{pb}^{-1}$ .

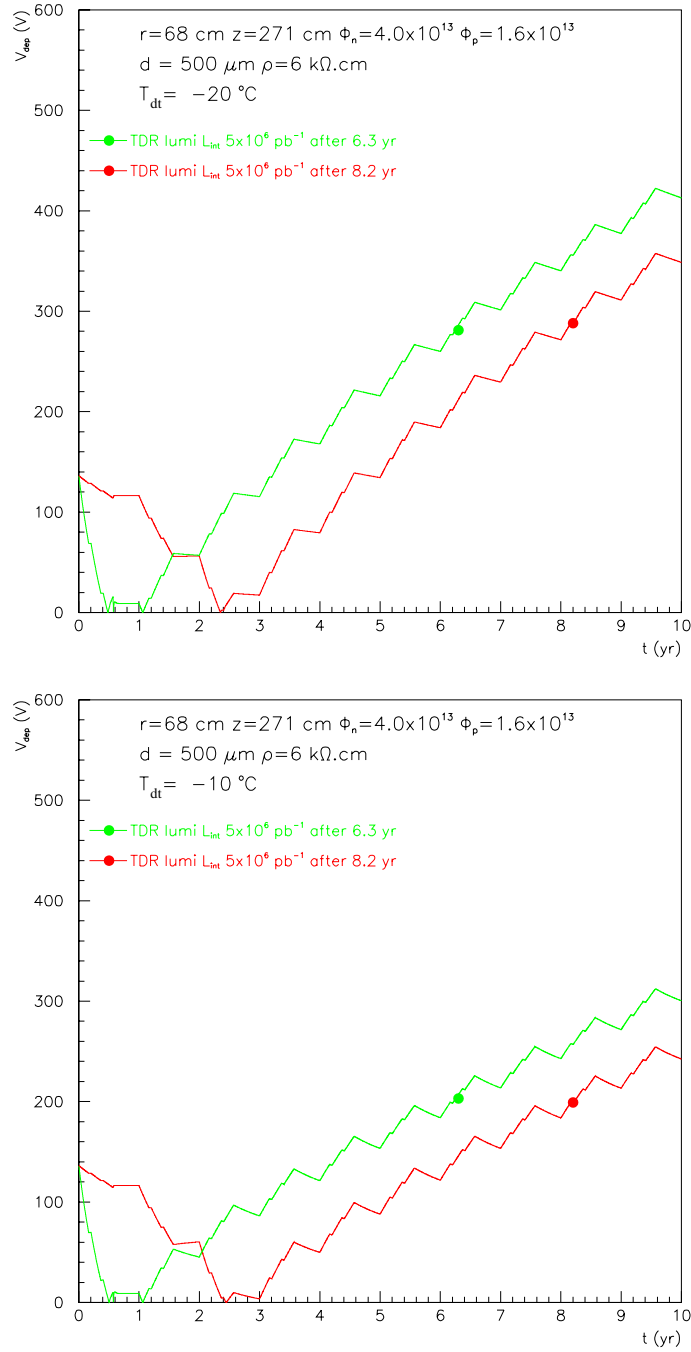


Figure 8: Depletion voltage as a function of time for a sensor in the hottest point of the Outer Endcap with one intervention after 1 year of data-taking (cf. table 14) and for two different luminosity scenarios (see text). Data-taking temperature  $T_{dt} = -20^\circ\text{C}$  (top) and  $T_{dt} = -10^\circ\text{C}$  (bottom). Dots correspond to  $5 \times 10^5\text{pb}^{-1}$ .

year(s) of the intervention	$T_{dt} = -20^\circ\text{C}$		$T_{dt} = -10^\circ\text{C}$	
	Barrel	Endcap	Barrel	Endcap
1	205	290	145	200
1+3	200	280	145	205
1+5	185	255	150	210
1+7	160	220	150	210
1+3+5	185	260	155	215
1+3+7	160	225	155	215
1+3+5+7	170	235	160	225

Table 14: Outer Tracker:  $V_{dep}$  (in V) after  $5 \times 10^5 \text{pb}^{-1}$  for different intervention scenarios.

year(s) of the intervention	$\rho$ k $\Omega\text{cm}$	$T_{dt} = -20^\circ\text{C}$		$T_{dt} = -10^\circ\text{C}$	
		Barrel	Barrel	Barrel	Barrel
1	3.5	205		145	
	6	185		125	
1+3	3.5	200		145	
	6	180		125	
1+5	3.5	185		150	
	6	165		130	
1+7	3.5	160		150	
	6	140		130	
1+3+5	3.5	185		155	
	6	165		135	
1+3+7	3.5	160		155	
	6	145		135	
1+3+5+7	3.5	170		160	
	6	150		140	

Table 15: Outer Tracker:  $V_{dep}$  (in V) after  $5 \times 10^5 \text{pb}^{-1}$  for different intervention scenarios, for the resistivity indicated in the second column.

## 8 Leakage current and power dissipated

The value of the leakage current represents the other fundamental issue for the choice of the operating temperature of the silicon. The increase  $\Delta j_V$  of the leakage current density after the sensor received a dose  $\Delta\Phi$  is proportional to the dose itself:

$$\Delta j_V = \alpha \Delta\Phi$$

After irradiation the leakage current benefits of annealing effects in a similar way as the effective charge carriers concentration does. No long term reverse annealing has been observed so far. The parametrization used to describe the annealing behaviour was:

$$\alpha(t, T) = \alpha_\infty \frac{g(\Theta(T) \cdot t)}{g(\infty)} \quad (5)$$

where  $g(t')$  was expressed as a sum of 6 exponentials terms:

$$g(t') = \sum_{i=1}^6 a_i e^{-\frac{t'}{\tau_i}}$$

The parameters used in the simulation are shown in table 20. Temperature dependence is introduced in eq. 5 by

$$\Theta(T) = e^{\frac{E_I}{k_B} \left( \frac{1}{T_{ref}} - \frac{1}{T} \right)}$$

where  $E_I = 1.09 \pm 0.03$  eV. The  $\alpha$  given by this set of parameter refers to  $T_{ref} = +21^\circ\text{C}$ . Therefore the real temperature of the sensor was obtained by scaling:

$$j_V(T) = j_V(T_{ref}) \left( \frac{T}{T_{ref}} \right)^2 \exp \left[ -\frac{E_g}{2k_B} \left( \frac{1}{T} - \frac{1}{T_{ref}} \right) \right]$$

with  $E_g = 1.24$  eV.

The leakage current behaviour was simulated for this study subdividing the total fluence in “radiation chunks”  $\Delta\Phi$ , in the same way as done in the case of the  $\Delta N_{eff}$  study.

Figures 9 and 10 show depletion voltage, leakage current and dissipated power during the LHC run, for sensors in the hottest points of Inner and Outer Tracker, in the case of data taking temperatures of  $T_{dt} = T_{sd} = -20^\circ\text{C}$  and  $T_{dt} = T_{sd} = -10^\circ\text{C}$  assuming no intervention is required. Figure 11 shows the total power dissipated in the silicon strip sensors of the Tracker always at  $T_{dt} = T_{sd} = -20^\circ\text{C}$  and  $T_{dt} = T_{sd} = -10^\circ\text{C}$  and assuming no intervention. The power dissipated in the case of  $T_{dt} = -20^\circ\text{C}$  is roughly 60 % of that at  $T_{dt} = -10^\circ\text{C}$ . This suggests that probably the best operation scenario is data taking at  $T_{dt} = -20^\circ\text{C}$  followed by shutdown periods at higher temperature.

## 9 Summary

The full depletion voltage for the silicon sensors required during the LHC run was evaluated on the basis of the so-called Hamburg Model. The hottest modules of the Inner (barrel/endcap) and Outer (barrel/endcap) Tracker were investigated for two data-taking temperatures,  $T_{dt} = -20^\circ\text{C}$  and  $T_{dt} = -10^\circ\text{C}$ , and in the conservative case of the highest substrate resistivity allowed. From the simulation the following results can be drawn:

1. values of  $V_{dep} < 400$  V are obtained in all the intervention scenarios examined in the case of the Inner Tracker (cf. table 8) and  $V_{dep} < 300$  V in the case of the Outer Tracker (cf. table 14);
2. as an example, for a realistic scenario with data-taking at  $T_{dt} = -20^\circ\text{C}$  ( $T_{dt} = -10^\circ\text{C}$ ) and two interventions, each consisting of 21 days at  $+20^\circ\text{C}$  and of 14 days at  $+10^\circ\text{C}$ , after the first and the fifth year of operation, i.e. at the beginning and at half the experiment lifetime, the depletion voltage required at the goal luminosity of  $5 \times 10^5 \text{pb}^{-1}$  in the hottest points of the Tracker will be: 330 V (275 V) for the Inner Barrel, 285 V (235 V) for the Inner Endcap, 185 V (150 V) for the Outer Barrel and 255 V (210 V) for the Outer Endcap;
3. beneficial annealing is reduced if sensors are kept at  $T_{dt} = -20^\circ\text{C}$  during data taking, but the power dissipated in the silicon is however about 60 % compared to the case of  $T_{dt} = -10^\circ\text{C}$ ;
4. sensor temperatures, during the shutdowns before type inversion is reached, in the range  $-20, +20^\circ\text{C}$  result in  $\Delta V_{dep} = 10 - 20$  V after  $5 \times 10^5 \text{pb}^{-1}$ .

Different running conditions of LHC, i.e. high luminosity since the first year of operations, do not affect substantially these conclusions. For the sensors of the Outer Tracker the spread of the initial substrate resistivity leads to a spread of the final  $V_{dep}$  of about 20 V while essentially no effect is observed for those of the Inner. Uncertainties on the model parameters used for the annealing could shift the result of about  $\pm 50$  V. This uncertainty can be reduced by monitoring the parameters on the sensors actually used in the experiment. The current uncertainties in the fluence can boost considerably the final  $V_{dep}$  especially in the case of the data-taking temperature  $T_{dt} = -20^\circ\text{C}$ , where no beneficial annealing is present. However the monitoring of the real radiation level, i.e. the factor between luminosity and fluence, will be possible during the data-taking using the leakage current of the sensors. This will be possible already since the early stages of the data-taking, when the absorbed dose is still small, and it will be an essential ingredient for the fine tuning of the sensors temperature in the Tracker.

## Acknowledgments

I would like to thank Michael Moll for the clear explanations on the Hamburg model.

## References

- [1] **CERN/LHCC 2000-9 (1999)**, The RD48/ROSE Collaboration, "*3<sup>rd</sup> RD48 Status Report*".
- [2] **CERN/LHCC 98-6 (1998)**, The CMS Collaboration, "*The Tracker Project Technical Design Report*".
- [3] **DESY-THESIS 1999-40 (1999)**, M.Moll, "*Radiation Damage in Silicon Particle Detectors*".
- [4] **CERN/LHCC 2000-16 (2000)** The CMS Collaboration, "*Addendum to the CMS Tracker TDR*".

year(s) of the intervention	$T_{dt} = -20^\circ\text{C}$		$T_{dt} = -10^\circ\text{C}$	
	Barrel	Endcap	Barrel	Endcap
1	360	305	270	230
1+3	340	290	280	240
1+5	300	255	285	240
1+3+5	315	265	300	255

Table 16: Inner Tracker:  $V_{dep}$  (in V) after  $5 \times 10^5 \text{pb}^{-1}$  for different intervention scenarios in the case of full nominal LHC luminosity  $0.5 \times 10^{35} \text{cm}^{-2} \text{s}^{-1}$  already in the first year of operations.

year(s) of the intervention	$T_{dt} = -20^\circ\text{C}$		$T_{dt} = -10^\circ\text{C}$	
	Barrel	Endcap	Barrel	Endcap
1	200	280	145	205
1+3	185	260	155	215
1+5	165	230	155	215
1+3+5	170	240	160	225

Table 17: Outer Tracker:  $V_{dep}$  (in V) after  $5 \times 10^5 \text{pb}^{-1}$  for different intervention scenarios in the case of full nominal LHC luminosity  $0.5 \times 10^{35} \text{cm}^{-2} \text{s}^{-1}$  already in the first year of operations.

year(s) of the intervention	$T_{dt} = -20^\circ\text{C}$				$T_{dt} = -10^\circ\text{C}$			
	$\Phi_n \times 2$ $\Phi_p \times 1$		$\Phi_n \times 1$ $\Phi_p \times 1.3$		$\Phi_n \times 2$ $\Phi_p \times 1$		$\Phi_n \times 1$ $\Phi_p \times 1.3$	
	Barrel	Endcap	Barrel	Endcap	Barrel	Endcap	Barrel	Endcap
1	+70	+70	+90	+70	+45	+50	+65	+50
1+3	+65	+70	+85	+70	+45	+50	+65	+55
1+5	+60	+60	+85	+65	+50	+45	+70	+55
1+7	+50	+55	+70	+60	+50	+50	+70	+55
1+3+5	+65	+60	+85	+65	+50	+55	+70	+55
1+3+7	+70	+55	+90	+60	+50	+50	+70	+55
1+3+5+7	+55	+60	+80	+65	+50	+45	+70	+60

Table 18: Inner Tracker:  $\Delta V_{dep}$  (in V) after  $5 \times 10^5 \text{pb}^{-1}$  due to the uncertainties on the fluence and for different scenarios of intervention.

year(s) of the intervention	$T_{dt} = -20^\circ\text{C}$				$T_{dt} = -10^\circ\text{C}$			
	$\Phi_n \times 2$ $\Phi_p \times 1$		$\Phi_n \times 1$ $\Phi_p \times 1.3$		$\Phi_n \times 2$ $\Phi_p \times 1$		$\Phi_n \times 1$ $\Phi_p \times 1.3$	
	Barrel	Endcap	Barrel	Endcap	Barrel	Endcap	Barrel	Endcap
1	+105	+200	+35	+30	+70	+135	+25	+20
1+3	+105	+195	+35	+30	+75	+140	+25	+20
1+5	+95	+180	+30	+30	+75	+145	+25	+25
1+7	+80	+155	+25	+25	+80	+145	+30	+25
1+3+5	+95	+180	+45	+30	+75	+145	+25	+20
1+3+7	+85	+160	+30	+25	+75	+145	+25	+25
1+3+5+7	+85	+165	+30	+30	+85	+155	+30	+25

Table 19: Outer Tracker:  $\Delta V_{dep}$  (in V) after  $5 \times 10^5 \text{pb}^{-1}$  due to the uncertainties on the fluence and for different scenarios of intervention.

$i$	$a_i$	$\tau_i$ (min)
1	0.156	$1.78 \times 10^1$
2	0.116	$1.19 \times 10^2$
3	0.131	$1.09 \times 10^3$
4	0.201	$1.48 \times 10^4$
5	0.093	$8.92 \times 10^4$
6	0.303	$\infty$

Table 20: Parameters for the annealing of leakage current used this simulation.

Inner Barrel  $\phi_n = 3.3 \times 10^{13} \text{ cm}^{-2}$   $\phi_p = 12.6 \times 10^{13} \text{ cm}^{-2}$

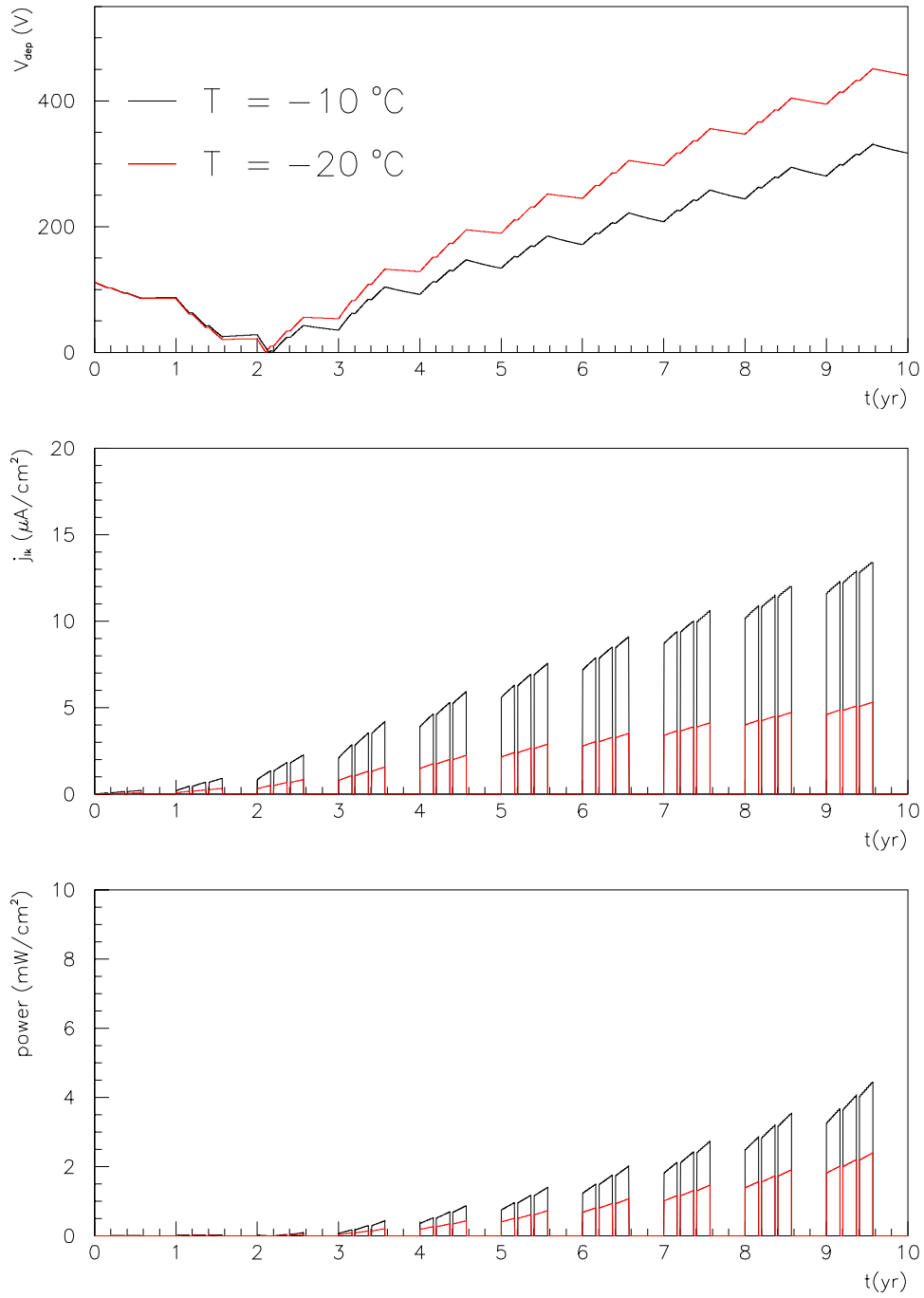


Figure 9: Depletion voltage (top), leakage current (centre) and dissipated power (bottom) as a function of time for a sensor in the hottest point of the Inner Barrel ( $\rho = 3 \text{ k}\Omega\text{cm}$ ,  $d = 320 \mu\text{m}$ ) in the case of no intervention during 10 years of LHC.

Outer Barrel  $\phi_n = 2.1 \times 10^{13} \text{ cm}^{-2}$   $\phi_p = 1.8 \times 10^{13} \text{ cm}^{-2}$

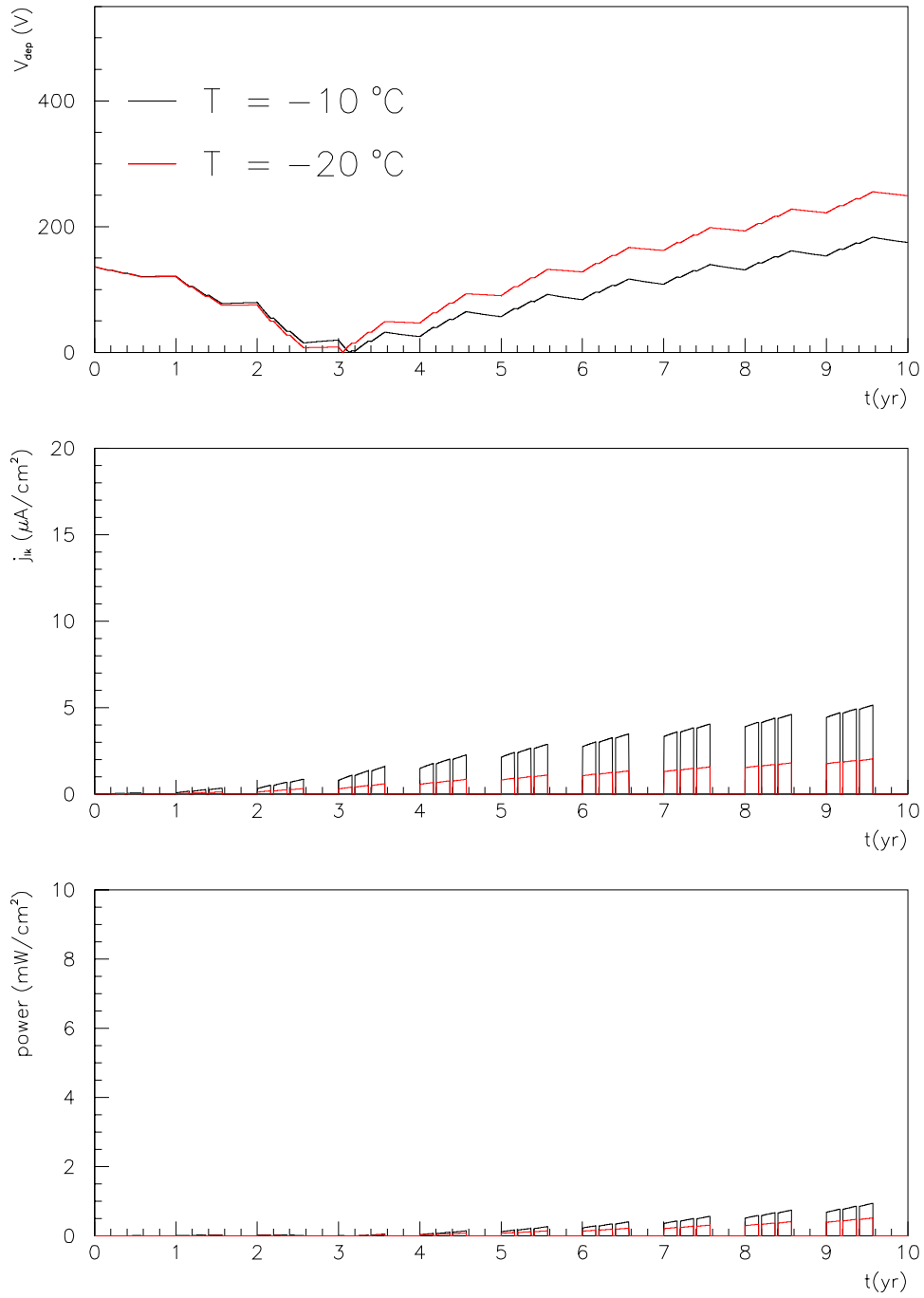


Figure 10: Depletion voltage (top), leakage current (centre) and dissipated power (bottom) as a function of time for a sensor in the hottest point of the Outer Barrel ( $\rho = 6 \text{ k}\Omega\text{cm}$ ,  $d = 500 \mu\text{m}$ ) in the case of no intervention during 10 years of LHC.

# Total Power Dissipated in Silicon Sensors

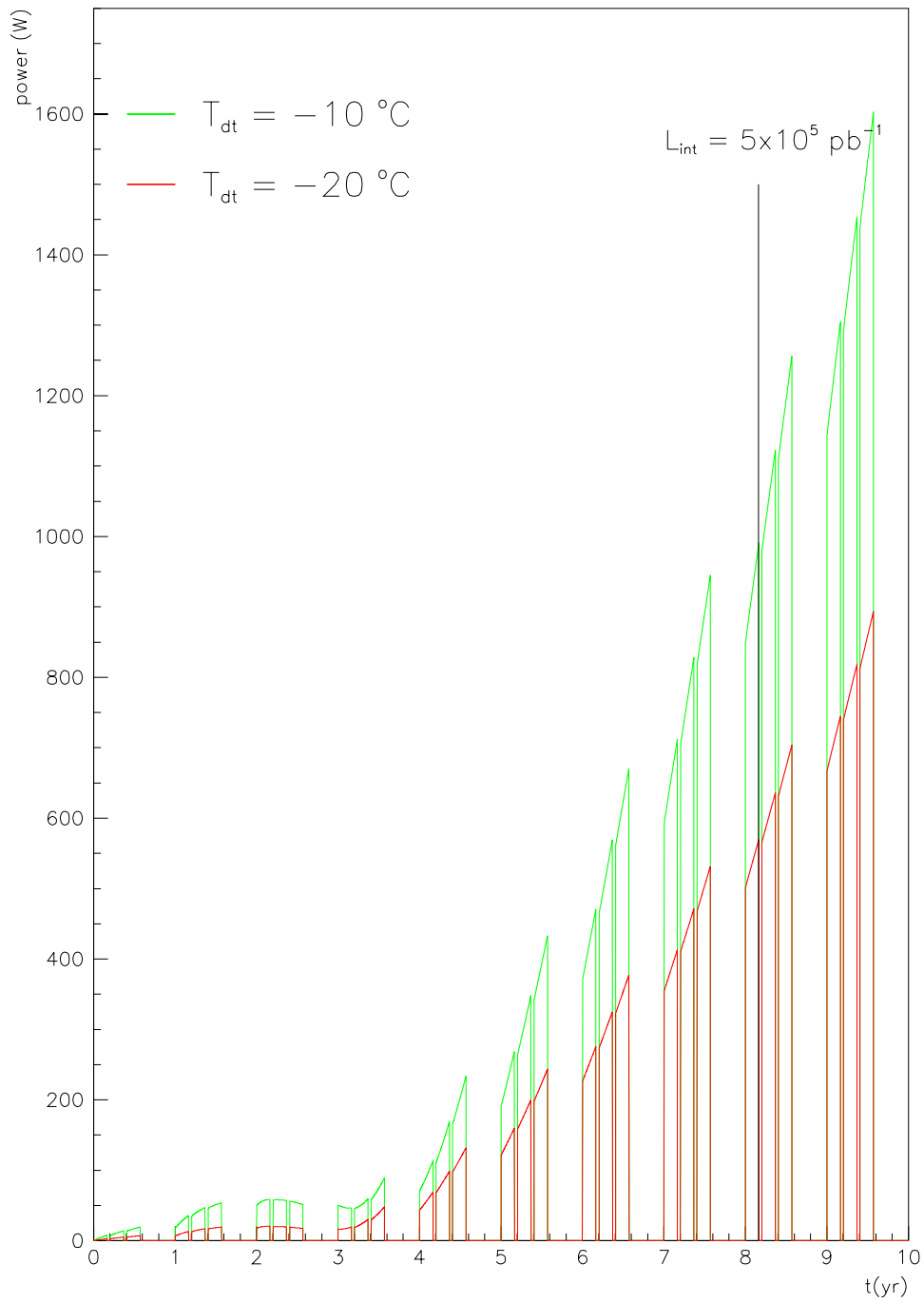


Figure 11: Total power dissipated in the silicon sensors of the CMS Tracker as a function of time in the case of no intervention during 10 years of LHC.